AJNR

Normal Venous Anatomy of the Brain: Demonstration with Gadopentetate Dimeglumine in Enhanced 3-D MR Angiography

Donald W. Chakeres, Petra Schmalbrock, Martha Brogan, Chun Yuan and Lance Cohen

AJNR Am J Neuroradiol 1990, 11 (6) 1107-1118
http://www.ajnr.org/content/11/6/1107

Normal Venous Anatomy of the Brain: Demonstration with Gadopentetate Dimeglumine in Enhanced 3-D MR Angiography

Donald W. Chakeres[1]
Petra Schmalbrock[2]
Martha Brogan[1]
Chun Yuan[2]
Lance Cohen[1]

This investigation evaluates whether gadopentetate dimeglumine enhancement of three-dimensional (3-D) acquisition MR angiography can generate clinically useful images of the normal venous anatomy of the brain. 3-D MR angiography of normal cerebral arterial anatomy has made rapid progress, although demonstration of detailed venous anatomy with similar techniques has been much less revealing. To overcome the limitation of slow venous flow, IV gadopentetate dimeglumine contrast enhancement was used to alter the relaxation times of blood, thus augmenting the venous signal. Several groups of patients were evaluated: we studied eight patients both with and without contrast enhancement, 20 patients and volunteers with multiple techniques to determine optimal technical parameters, and seven patients in whom enhanced MR studies were compared with standard selective biplane cut-film arterial angiograms. Only the large dural sinuses (such as the transverse sinus) could be seen on unenhanced studies owing to the saturation of slowly flowing venous spins. With contrast enhancement, many of the important small and large cerebral venous structures were routinely seen with reasonable scanning times (7 min). The venous anatomy was well seen for approximately one-half hour after injection and correlated well with angiograms. There are several important limitations to this technique, including a limited field of view, variable visibility of specific veins owing to technical and physiologic factors, confusion of enhancing non–flow-related structures, and lack of detailed physiologic information.

Single excitation 3-D MR angiograms are insensitive in the evaluation of cerebral venous structures. Enhancement with gadopentetate dimeglumine affords rapid scanning and excellent visualization of the pertinent venous anatomy. The best image quality was obtained with a sequence of 50/7/30° (TR/TE/flip angle).

AJNR 11:1107–1118, November/December 1990; *AJR* 156: January 1991

A number of MR angiographic techniques have been proposed that use the advantages of flowing blood to differentiate moving from stationary spins. The two most common techniques are based on time-of-flight effects of moving spins or on motion-induced phase shifts [1–7]. The most time-efficient methods are those that use three-dimensional (3-D) volume and multiple thin two-dimensional (2-D) [8, 9] time-of-flight techniques, since they use only single excitation data and there is no need to subtract different data sets. Subtraction of 3-D MR angiograms with and without gadopentetate dimeglumine has been reported to improve visualization of the venous structures (Seider M, unpublished data). Phase-contrast MR angiographic techniques evaluate differences in phase induced by motion in the presence of magnetic field gradients [5]. 3-D volume phase-contrast techniques generally have long acquisition times, up to 40 min.

The 3-D time-of-flight volume MR angiographic technique has made rapid progress in the acquisition of images of normal cerebral arterial anatomy, yielding good correlation with standard angiography [10–13]; however, demonstration of detailed venous anatomy has been much less revealing. Only large venous structures such as the dural sinuses are seen routinely, and even then, not to the best advantage.

Received August 29, 1989; revision requested November 17, 1989; final revision received June 1, 1990; accepted June 4, 1990.

[1] Department of Radiology, Division of Neuroradiology, Ohio State University Hospital, Ohio State University College of Medicine, 410 W. 10th Ave., Columbus, OH 43210. Address reprint requests to D. W. Chakeres.

[2] General Electric Medical Systems, Milwaukee, WI 53201.

0195–6108/90/1106–1107

Noninvasive evaluation of the cerebral venous structures is desirable in order to ensure a complete evaluation of the brain vasculature. Venous thrombosis, stricture, compression, displacement, and anomalies are all important angiographic findings that ordinarily are not visible on images designed to optimize single-excitation 3-D volume MR angiographic arterial studies.

The poor visualization of the venous anatomy with the 3-D MR angiographic technique is partially a result of slower moving venous spins that are saturated within the imaging volume. To avoid this problem, we generated MR angiograms that were not based entirely on flow effects, but improved by relaxation time differences between vascular structures and stationary tissues. For this purpose, the contrast between blood and brain tissue was enhanced by IV injection of gadopentetate dimeglumine. Because this investigation was primarily focused on development of the technique and so many different parameters were varied, this article does not attempt to address the utility and accuracy of visualization of specific veins and abnormalities. It is a study specifically to review the technical parameters that are optimal for gadopentetate-dimeglumine–enhanced venous MR angiography.

Subjects and Methods

Thirty-five patients and volunteers 4–75 years old (mean age, 45 years) were evaluated. Almost all of the patients were adults. Images were acquired on a 1.5-T General Electric Signa system using a gradient-echo 3-D volume imaging sequence, which allows very short TEs (Schmalbrock P, unpublished data). The sequence uses first-order flow-motion compensation in both read- and slice-selection directions. The slice thickness can be varied from 0.7 to 5 mm, and the field of view from 16 to 48 cm. Initially, the shortest possible TE (<7 msec) required field-of-view restrictions in the frequency-encoded direction. Later versions of the pulse sequence code avoided this limitation. In most cases, 60 1.5-mm-thick slices were acquired with a field of view of 20–24 cm and a 128 × 256 matrix resolution. Because only a single acquisition is required, scan times were typically under 7 min. Thirty slices could be acquired in 3½ min.

Angiographic displays were generated by using ray-tracing methods on a stack of thin sections [5, 7, 14]. In the computational algorithm, parallel rays through a chosen imaging volume selected the points with maximum signal from the stack of individual images. In this fashion, a new projection image was generated. By changing the direction of the parallel rays, projection images of various angles could be generated. A minimum of six different projections were calculated for any chosen stack of slices. The projections were created to correspond to standard anteroposterior and lateral angiograms.

We initially obtained unenhanced images to evaluate the visualization of venous structures (Fig. 1). Then, we compared eight MR angiographic studies with and without IV gadopentetate dimeglumine enhancement (10 ml, 4.7 g) in the same patient or volunteer to evaluate the visualization of cerebral venous anatomy with enhancement (Fig. 2).

Varying T1 contrast weighting on unenhanced and contrast-enhanced images was achieved by manipulating the TR and flip angle.

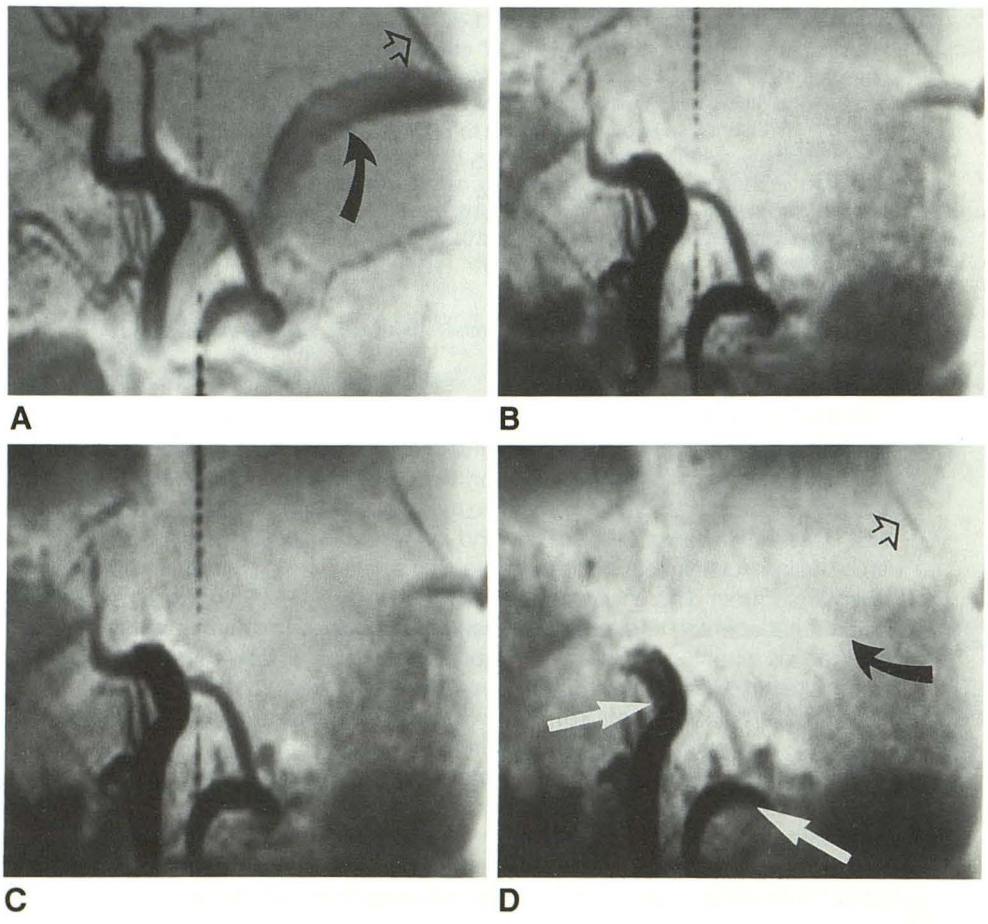

Fig. 1.—Effect of variable flip angle on unenhanced 3-D MR angiography.
***A–D*, Lateral projections from unenhanced axially acquired 3-D volume images, 50/7 (TR/TE), with variable flip angles of 15° (*A*), 30° (*B*), 45° (*C*), and 60° (*D*). Pixel size was 1.5 × 1.8 × 0.9 mm. Flow compensation was applied in both read- and slab-excitation directions. On lower-flip-angle image, visualization of venous structures, including transverse (*solid black arrows*) and straight (*open arrows*) sinuses, is faint. With larger flip angle, straight and transverse sinuses are almost completely absent. Even arterial structures (*white arrows*) are degraded by saturation effects.**

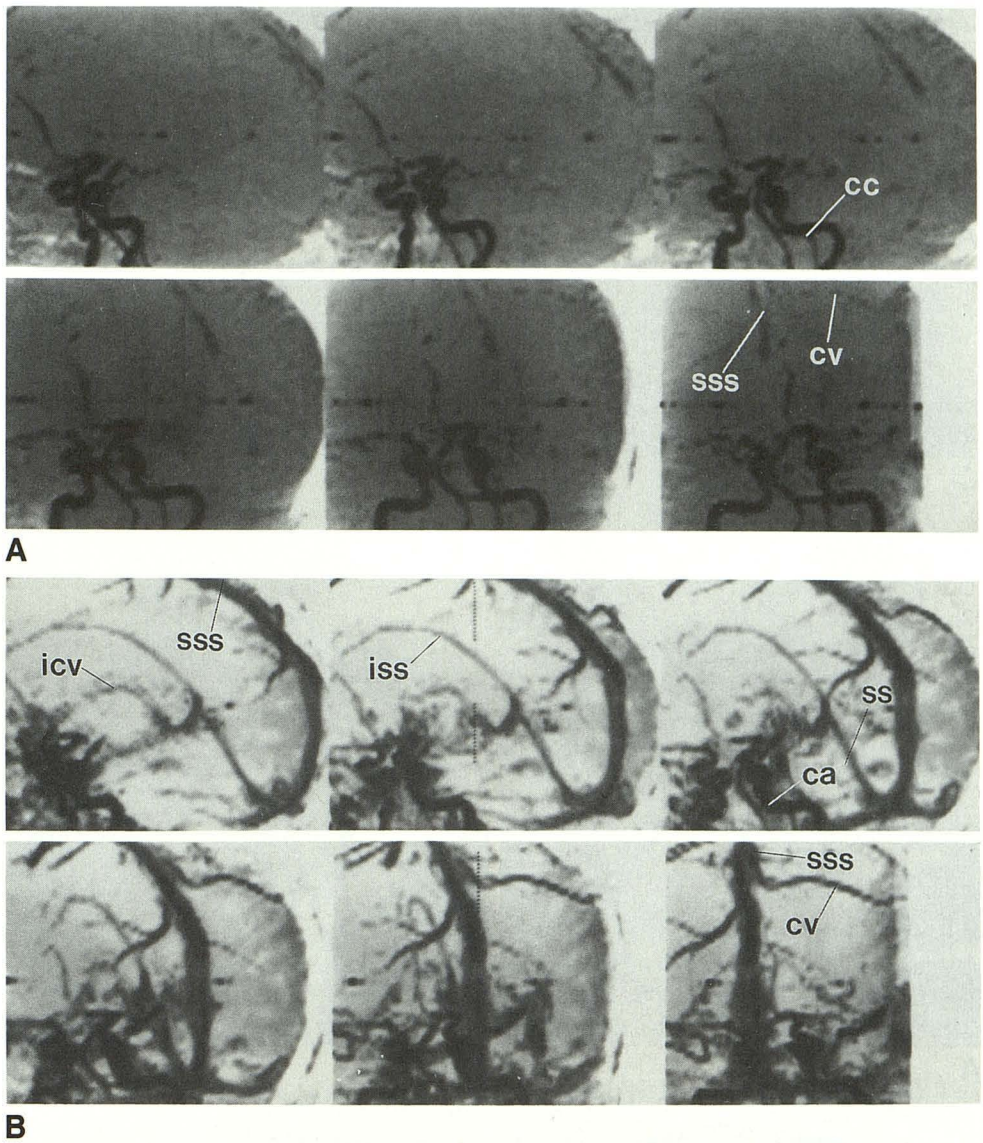

Fig. 2.—Multiple projections with and without contrast enhancement. 3-D MR angiograms, 47/7 (TR/TE), were acquired sagittally and are displayed in multiple projections (top left image is lateral; lower right is anteroposterior). Voxel size was 1.5 × 1.9 × 0.9 mm.

***A*, Unenhanced study, with a 15° flip angle, poorly displays venous anatomy, although proximal arterial system is visible.**

***B*, Enhanced study, with a 30° flip angle for optimal results, shows a dramatic improvement in visualization of many venous structures.**

cc = carotid canal, sss = superior sagittal sinus, cv = cortical vein, icv = internal cerebral vein, iss = inferior sagittal sinus, ca = carotid artery, ss = straight sinus.

Spoiler gradients on all axes allowed the generation of images that were more T1 weighted. We varied the TR from 33 to 50 msec. Initially, unenhanced MR angiograms with flip angles of 15°, 30°, 45°, and 60° were obtained in the same volunteer (Fig. 1). Then, similar series of images was obtained with gadopentetate dimeglumine in the same volunteer (Fig. 3).

The TE was varied from 7 to 14 msec to evaluate its effect on visualization of the veins, as well as fat suppression due to chemical shift [15].

To evaluate washout of contrast material over time, consecutive contrast-enhanced images in the same volunteer were completed (Fig. 4).

To evaluate the effect of section plane and image volume on venous visualization, consecutive section planes in the same volunteer were compared after contrast injection (Fig. 5).

A comparison was made of single- and multiple-image volume selection for ray-tracing projections (Fig. 6) and the original images were reviewed for anatomic detail (Fig. 7).

We directly compared standard selective biplane cut-film cerebral angiograms and MR angiograms from the same seven patients (Figs. 8–11). A general evaluation was made of the quality, extent of visualization of the venous system, artifacts, and optimal imaging parameters with cerebral venous MR angiography. Because the examinations were done with many different techniques, a detailed quantitative evaluation of specific veins or abnormalities with varying techniques was not possible.

Results

The unenhanced MR angiograms displayed the venous structures poorly (Fig. 1). The images with higher flip angles further limited venous visualization. Comparison of enhanced and unenhanced scans of adult patients was done as soon as possible after injection of gadopentetate dimeglumine. There was remarkable improvement in the visualization of the venous system with enhancement (Fig. 2). Most of the major venous structures were well seen. Visualization of the arterial structures was not significantly improved with contrast material.

Changes in T1 weighing did have a noticeable impact on image quality in both enhanced and unenhanced examina-

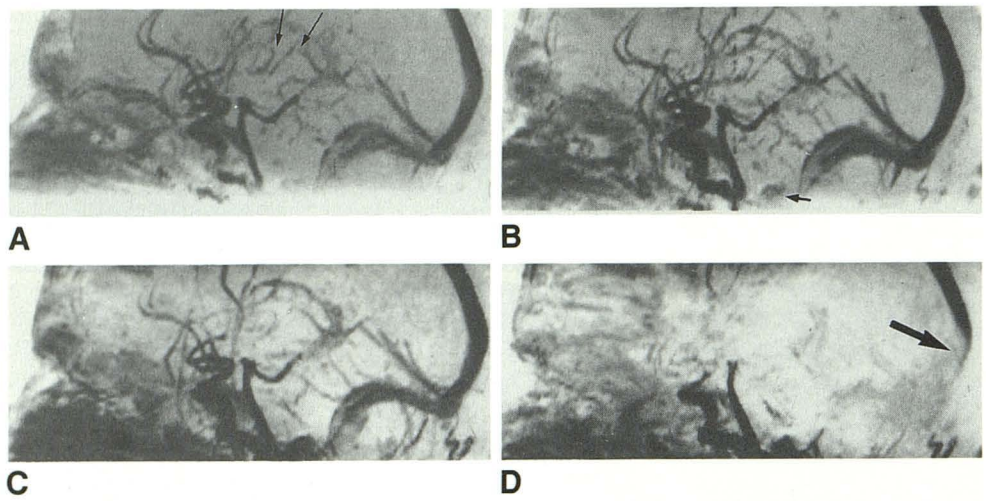

Fig. 3.—Variable-flip-angle contrast-enhanced MR angiograms.

***A–D*, Axially acquired images were obtained on two consecutive days to avoid changes related to contrast washout (*A* and *B*, one day; *C* and *D*, the next). The only acquisition parameter varied was the flip angle: 15° (*A*), 30° (*B*), 45° (*C*), and 60° (*D*). Images are displayed as lateral angiograms. Image with 60° flip angle (*D*) shows extensive saturation of superior sagittal sinus and transverse sinuses in inferior portion of image (*arrow*). Other images are of comparable quality, but there are subtle differences. Image with 15° flip angle (*A*) shows less detail of deep venous system (*arrows*). Original images showed less contrast between gray and white matter structures than did higher-flip-angle images. Choroid plexus is more prominent on image with 45° flip angle (*C*), leading to confusion with flowing structures. Enhancement of nasal mucosa is visible on all images.**

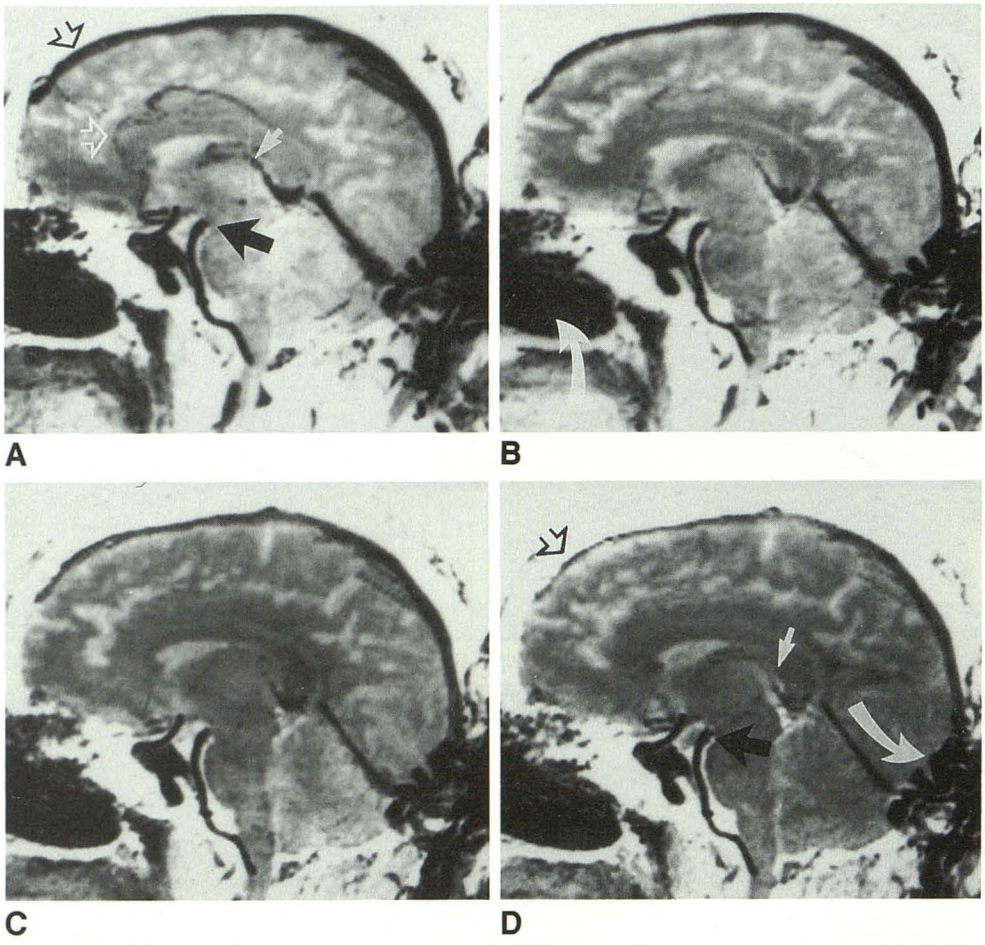

Fig. 4.—Time-related contrast washout.

***A–D*, Four consecutive sagittally acquired images, 50/11/30°, at 4 (*A*), 17 (*B*), 31 (*C*), and 44 (*D*) min after injection of 10 ml of gadopentetate dimeglumine. Voxel size was 1.5 × 1.6 × 0.8 mm. Only the central 22 images of a total of 60 were postprocessed for ray-tracing projection images shown. Best venous image contrast is seen on 4-min study (*A*). Midline venous structures, including superior sagittal sinus (*open black arrows*) and internal cerebral veins (*solid white arrows*), are seen well (*A*). A number of important arterial structures, including pericallosal (*open white arrow*) and basilar (*solid black arrows*) arteries, are seen on 4-min image also. With longer post-injection delays, smaller vascular structures are not seen as well (*D*). Venous quality of 44-min image (*D*) is marginal. There is minimal change in visualization of large arterial structures (*solid black arrows*) with time. Extensive enhancement of nasal mucosa and wraparound artifact is noted (*curved white arrows*).**

tions. Varying the TR from 33 to 50 msec did not significantly alter the results except for changing the total examination time. Longer TRs were not considered because of the prolonged examination time, and shorter TRs were not considered owing to technical limitations and expected decrease in signal to noise. On unenhanced studies with lower flip angles, only the large dural sinuses (such as the superior sagittal and transverse sinuses) could be seen (Fig. 1A). Owing to saturation of the slow-flowing venous spins, the larger the flip angle, the worse the venous visualization (Figs. 1B–1D). On

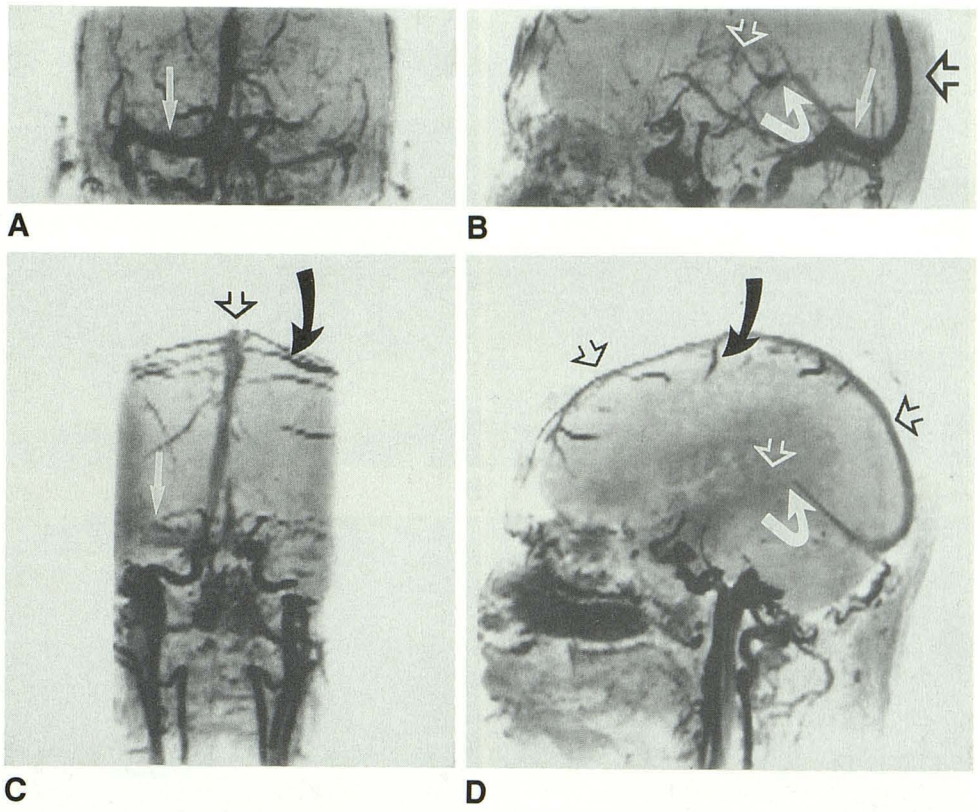

Fig. 5.—Comparison of axial and sagittal acquisitions.

***A–D*, Contrast-enhanced images, 52/11/30°, were obtained with both axially (*A* and *B*) and sagittally (*C* and *D*) acquired techniques, then postprocessed with ray tracing to generate similar anteroposterior (*A* and *C*) and lateral (*B* and *D*) projections. Each acquisition has advantages for visualization of specific vessels. Deep venous system is better seen on axially acquired series (*A* and *B*), including vein of Galen (*curved white arrows*), transverse sinus (*straight white arrows*), and internal cerebral veins (*open white arrow*). On sagittally acquired images (*C* and *D*), superior sagittal sinus (*open black arrows*), jugular fossa, and cortical veins (*curved black arrows*) are seen best.**

the contrast-enhanced studies, large flip angles also led to more venous saturation (Fig. 3). Increase in background signal from non–flow-related enhancing tissues (nasal mucosa and brain) became more pronounced with higher flip angles (Fig. 3D). A flip angle of approximately 30° was optimal, though there was a wide range that was adequate. The lower-flip-angle original images had less T1 weighting. The higher-flip-angle original images were less attractive.

The effect of the various TEs on image quality was important. No substantial signal loss for the venous structures was observed when increasing TEs from 7 to 15 msec. Modification of the TE between 7 and 11 msec, however, caused a variation in the background signal intensity of the fatty tissues (Fig. 7). Best results were obtained with a TE of 7 or 11 msec, where the magnetization of fat and water aligns in an antiparallel fashion, while a TE of 9–10 msec with parallel magnetization increased the background signal [15]. This was important in the suppression of unwanted signal from the scalp on the ray-tracing projection images.

The improvement in venous visualization lasted approximately 30 min after injection (Fig. 4). The sooner the examination followed the injection, the better the result, but the contrast load was adequate for at least two acquisitions.

Orientation of the acquisition section plane, slice thickness, and total number of slices were important factors, since they defined the total imaging saturation volume. When the imaging volume completely encompassed the majority of a venous territory, the results were compromised (Fig. 5). This indicates that the signal intensity is not entirely due to T1 contrast, but is also dependent on inflow effects. For example, rostral axial sections of the vertex did not demonstrate the superior sagittal sinus as well as a direct sagittal series did (Fig. 5A). However, the deep venous system was usually seen better on axial images that did not include the vertex of the brain than on direct sagittal images (Fig. 5B). Coronal acquisitions, though possible, were not frequently used since they did not correspond with the venous anatomy in terms of covering a wide area.

The angiographic ray-tracing projection generated from smaller processed volumes best demonstrated smaller structures (Fig. 6) [14]. The larger structures (for example, the superior sagittal sinus) were less sensitive to the size of the reconstructed volumes.

The original slice images were of good quality, with T1-weighted contrast similar to that of spin-echo images (Figs. 7 and 11). Diagnosis of soft-tissue disease was possible (Figs. 7 and 11). The images were not clearly better than standard spin-echo images; however, the thin slice thickness was advantageous in the visualization of small structures.

Comparison of the MR and standard angiograms confirmed that, on the enhanced images, many of the important cerebral venous structures were seen routinely. In most instances, MR angiography correlated well with standard selective cerebral angiography (Figs. 8–11), although the results varied among patients. Routinely visualized structures included superior and inferior sagittal sinuses (Fig. 2), transverse and sigmoid sinuses (Fig. 11), vein of Galen (Fig. 9), basal vein of Rosenthal (Fig. 9), internal cerebral and thalamostriate veins (Fig. 8), lateral mesencephalic and jugular veins (Fig. 5), and cortical veins (Figs. 5 and 6). Occasionally, the septal (Fig. 6), precentral cerebellar, and other smaller veins were visible. Contrast enhancement helped define the extent of disease in

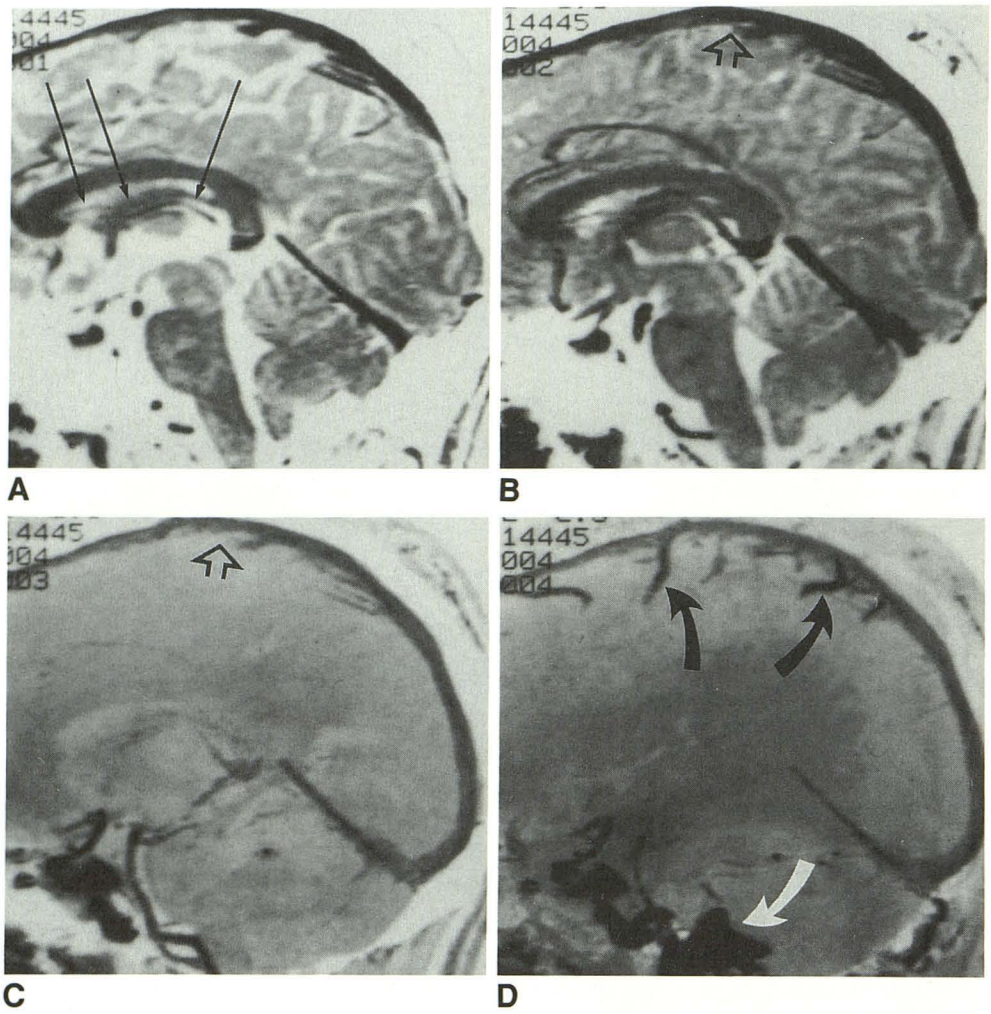

Fig. 6.—Effects of ray tracing postprocessing.

A–D, Four images generated from one set of contrast-enhanced sagittally acquired images, 52/11/30°, show effects of different postprocessing techniques on visualization of various venous structures. *A* is single midline section from imaging block. Visualization of even small veins, such as internal cerebral and septal veins (*straight solid arrows*), is superb. *B* was processed from central four images. *C* and *D* were processed from 22 and 60 images, respectively. Most smaller midline veins are not visible on thicker slabs (*C* and *D*). On large imaging block (*D*), cortical veins (*curved black arrows*), complete superior sagittal sinus (*open arrows*), and jugular fossa (*curved white arrow*) are better displayed than on narrow midline image.

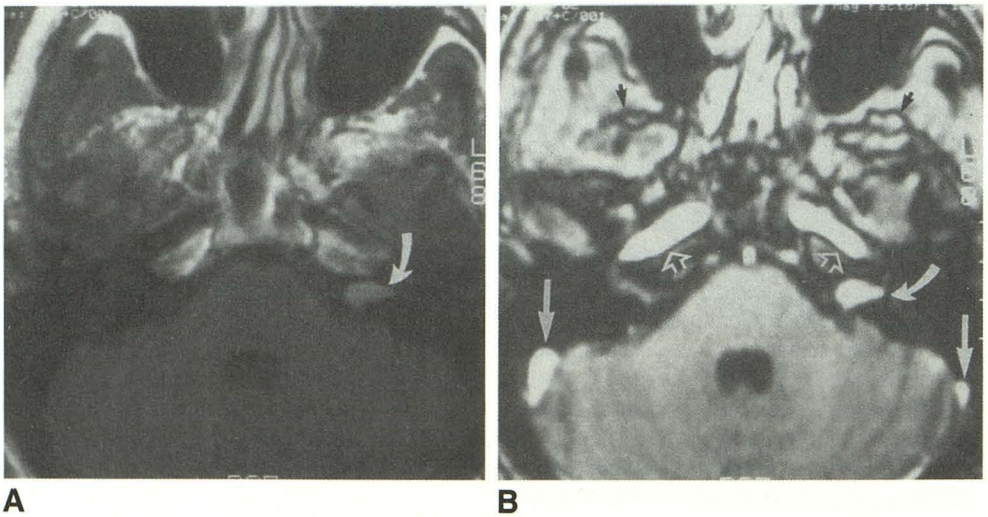

Fig. 7.—Comparison of spin-echo and 3-D images.

A and *B*, Gadopentetate-dimeglumine–enhanced axial images in patient with acoustic neuroma. Spin-echo image, 600/30, with a 256 × 256 matrix and 5-mm-thick section (*A*) and single 1.5-mm 256 × 128 section from a 60-slice 3-D MR angiogram, 47/11/30° (*B*), were compared. Both show enhancing intracanalicular mass on left (*curved arrows*). MR angiogram (*B*) shows high signal from carotid arteries (*open arrows*) and sigmoid sinuses (*solid straight white arrows*). Black interface of sub-temporal fossa fat and adjacent muscles is seen secondary to chemical-shift effect (*black arrows*).

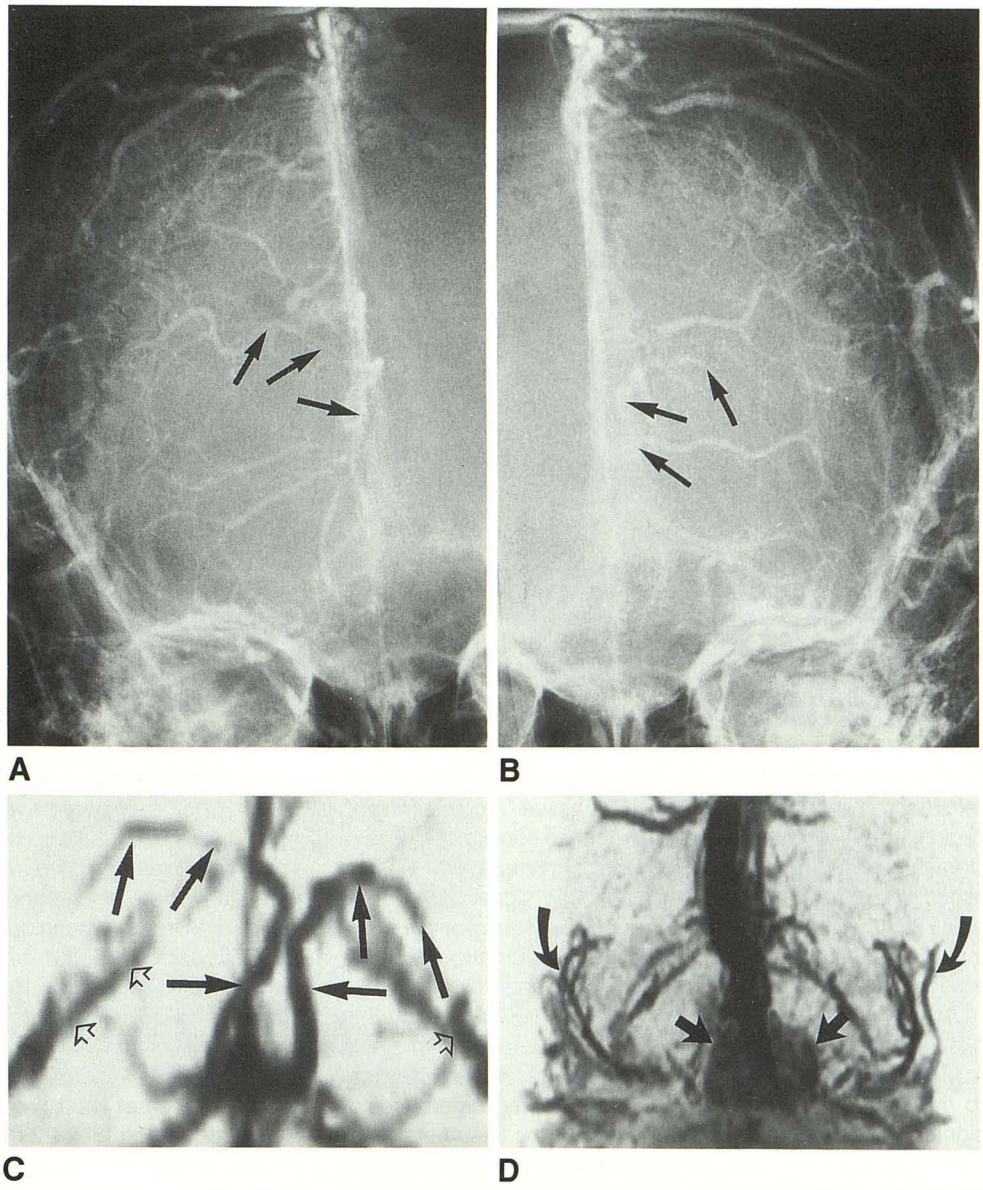

Fig. 8.—Direct comparison of anteroposterior standard and MR angiograms.

***A–D*, Standard cut-film selective bilateral anteroposterior common carotid angiograms (*A* and *B*) and axially acquired MR angiograms, 40/7/30°, ray-tracing projections (*C* and *D*). Only central volume of brain surrounding deep venous system was processed on *C* to better display deep venous anatomy. Complete volume was processed on *D*. An enhancing suprasellar craniopharyngioma is seen (*straight arrows*, *D*). Mild subfalcine herniation to left is seen by distortion of internal cerebral and thalamostriate veins (*solid arrows*, *A–C*). MR angiogram (*C*) accurately reflects local distortion. Complete data reconstruction on *D* shows superior sagittal sinus and middle cerebral arteries (*curved arrows*) better. Choroid plexus of lateral temporal horns is seen also (*open arrows*, *C*).**

cases of an arteriovenous malformation (Fig. 10), acoustic neuroma (Fig. 7), and metastatic tumor obstructing the jugular vein (Fig. 11).

Discussion

Most MR angiographic techniques exploit one of two strategies to obtain sensitivity to flowing blood. The first strategy relies on changes in the phase of the transverse magnetization, which are introduced when blood moves in the presence of magnetic field gradients. Those spins moving in the direction of increasing gradient strength will advance in phase, while those moving in the opposite direction will fall behind the phase of stationary tissue. Phase-sensitive techniques usually involve subtraction of data obtained with different gradient schemes, such as bipolar gradient pairs [4], with and without first-order motion compensation [3], or use of different first-moment magnetic field gradients (Pelc NJ, unpublished data). Investigation of complex blood flow requires acquisition of three separate data sets for the three gradient directions, thus leading to long examination times (up to 40 min). Since the changes in the phases are directly related to the velocity of flow, physiologic information can be obtained. Phase-sensitive techniques are capable of detecting relatively slow flow over large fields of view, since they are less sensitive to saturation. They are sensitive only to the component of flow coincident with the direction of the applied magnetic field gradient. For routine clinical studies they are very slow, partially because multiple acquisitions are needed. Because of the multiple acquisitions, high-resolution studies take even longer. We initiated our study to find technical parameters that would eliminate as many of these limitations as possible.

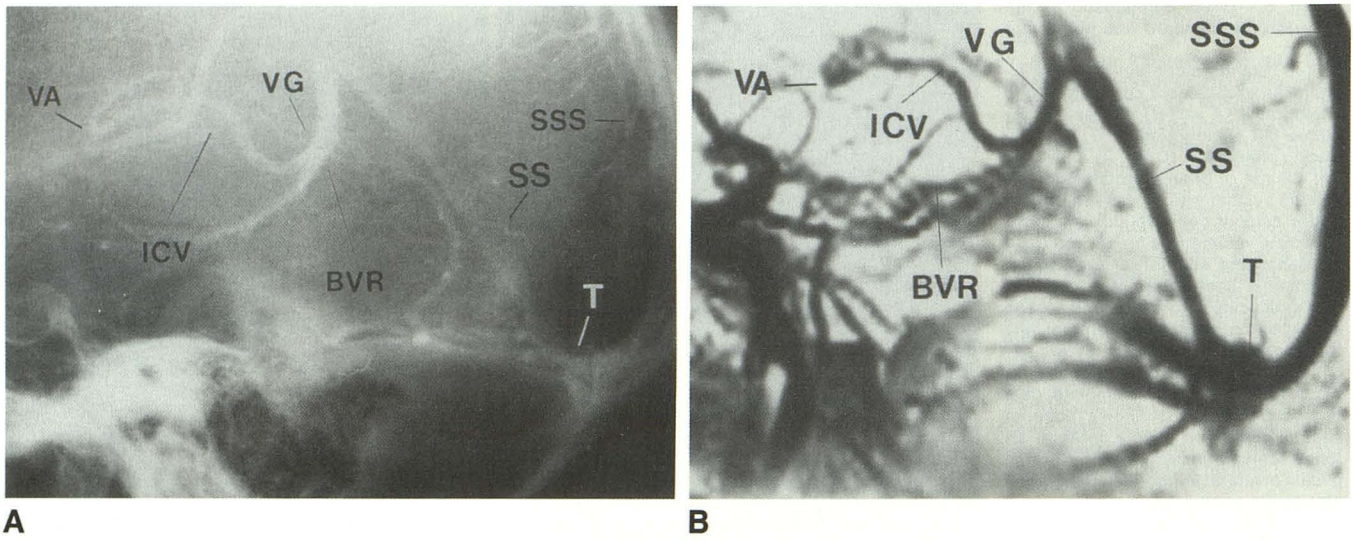

Fig. 9.—Direct comparison of a lateral standard and MR angiograms.
***A*, Standard cut-film selective carotid lateral angiogram shows much of deep venous system.**
***B*, Corresponding axially acquired MR angiogram, postprocessed lateral projection.**
Deep venous system is well seen on both studies. Carotid arteries are well seen. VA = venous angle, ICV = internal cerebral vein, VG = vein of Galen, BVR = basal vein of Rosenthal, SSS = superior sagittal sinus, SS = straight sinus, T = torcular Herophili.

The second MR angiographic strategy relies on time-of-flight effects to transport flowing spins with a different RF excitation history than the stationary tissue into the imaging region. The different excitation history can consist of selective presaturation [16] or inversion pulses (Wright GA, unpublished data), which are used to "tag" the signal of inflowing spins. Another time-of-flight technique takes advantage of the inflow of "fresh" unsaturated spins in a volume of saturated stationary spins, as in 2-D and 3-D time-of-flight angiography.

Acquisition of a single 2-D time-of-flight MR angiogram that highlights the signal from moving spins is possible in just a few seconds. The direction of flow should be perpendicular to the section plane for ideal results. Marked differences in signal between moving spins and stationary tissue are common with this technique. Flow parallel to the section plane can induce saturation. The original 2-D MR angiograms are of poor quality with respect to anatomic detail, since the signal of the stationary tissue has a poor signal-to-noise ratio. Also, the resolution (slice thickness) is limited by gradient strength. To create a ray-tracing projection, multiple images are needed, increasing the acquisition time. Motion between sections can degrade image quality [9], similar to CT postprocessing artifacts. The time-of-flight methods also are limited to the investigation of relatively fast flow (arteries or high-velocity veins) and/or small imaging regions, since the inflow of initially "fresh" spins is rapidly saturated as the imaging volume is traversed. For example, slow moving spins in the internal cerebral veins would be more saturated with sagittal than with coronal images. These differences can produce regions of low signal that are not related to a true stenosis. Because of the limitations of 2-D MR angiographic techniques, we decided to investigate the visualization of the venous anatomy with our techniques.

Other investigators have reported early results on the use of gadopentetate dimeglumine with 3-D MR angiographic time-of-flight imaging techniques (Seiderer M, unpublished data). They subtracted two separate series of 3-D MR angiograms before and after contrast enhancement. It was found that visualization of the venous system was particularly improved. It was also reported that the anatomic information obtained with this technique was comparable to that obtained with digital subtraction angiography. The optimal technical parameters were similar to those we concluded to be optimal, 33/11/40° (TR/TE/flip angle); however, their technique has several major drawbacks: patient motion during or between the two series seriously degraded image quality, the acquisition time was at least twice that of a single acquisition, and each acquisition took 22 min.

We wished to develop a clinically useful single fast-acquisition MR angiographic technique that would provide high-resolution quality on the original and ray-tracing images. It was clear from prior experience with T1-weighted spin-echo imaging that the veins enhanced intensely following injection of contrast material. We attempted to take advantage of this phenomenon with a 3-D MR angiographic technique. Our approach can be classified as a hybrid time-of-flight T1-weighted method. We use a 3-D pulse sequence variation that could be used for arterial studies, but it is more T1 weighted. The 3-D techniques include high resolution with slice thickness potentially thinner than with 2-D MR angiography, short acquisition times (30 sections in 3½ min), and excellent original T1-weighted images owing to the improved signal-to-noise ratio of the 3-D MR angiographic technique.

This study demonstrates that unenhanced single-excitation 3-D MR angiography is an insensitive examination for demonstrating venous anatomy (Fig. 1). The venous flow rates in even the large dural sinuses are much slower than the arterial rates; thus, the spins reach saturation before they exit the

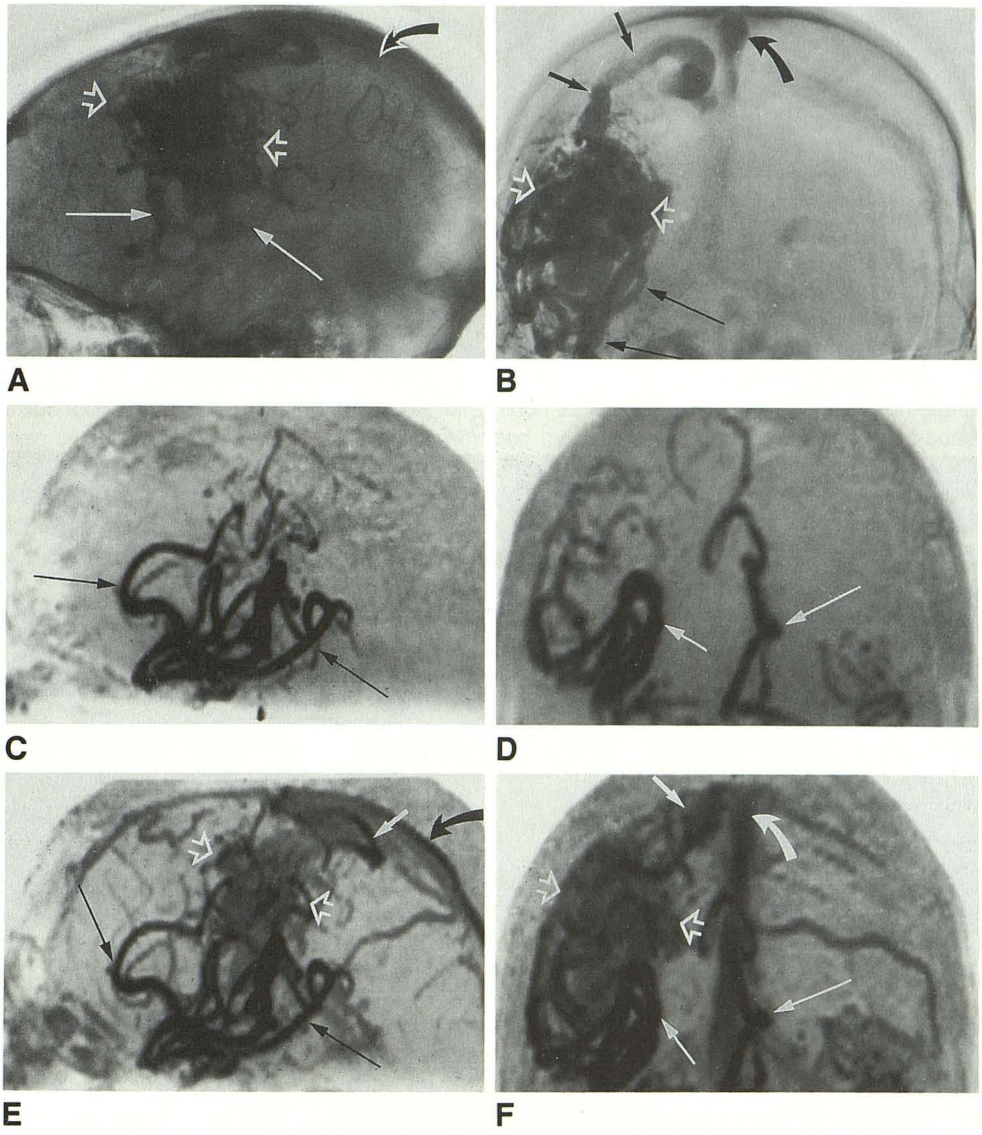

Fig. 10.—Comparison of standard and MR angiograms in patient with frontoparietal arteriovenous malformation (AVM) demonstrates importance of contrast enhancement.

***A* and *B*, Lateral (*A*) and anteroposterior (*B*) late arterial right carotid artery angiograms show large AVM (*open arrows*). Large arterial feeders (*long thin arrows*). Huge dilated draining veins (*shorter straight arrows*) are seen coursing superiorly to empty into superior sagittal sinus (*curved arrows*).**

***C* and *D*, Unenhanced 3-D MR angiograms, 47/11/30°, lateral (*C*) and anteroposterior (*D*) ray-tracing images, display enlarged arterial feeders from anterior and middle cerebral arteries (*arrows*) toward AVM. AVM and its large draining veins, however, are not visible.**

***E* and *F*, Contrast-enhanced 3-D MR angiograms, 47/11/30°, lateral (*E*) and anteroposterior (*F*) ray-tracing images, better display large cluster of draining veins (*solid white arrows*). Without contrast enhancement, complete extent of abnormality would be underestimated.**

imaging slab. This is particularly the case for thick-volume slabs, short TRs, and higher flip angles (Fig. 1). Very little significant clinical information relating to the venous system was generated from 3-D MR angiographic techniques used for optimal arterial visualization. The limited visualization of the veins is not a disadvantage if the goal is to display the arteries only.

To overcome the limitations of unenhanced single-excitation 3-D MR angiography, we demonstrated that contrast enhancement markedly improves venous visualization by altering the relaxation times of venous blood rather than relying solely on rapid flow velocities (Figs. 2–11). Because an intact blood-brain barrier excludes contrast material from the brain, there is limited enhancement of the brain itself (Figs. 2 and 3). The contrast agent was concentrated in the blood pool, causing large changes in the relaxation times of the venous blood in comparison with the surrounding brain. This technique may not be useful outside of the brain. The image contrast for arterial structures was not significantly altered with gadopentetate dimeglumine, since the signal generated by rapid flow-related enhancement alone produces nearly maximum contrast (Fig. 2).

The degree of T1 weighting was an important factor affecting venous visualization. The short T1 relaxation time of blood following enhancement allows for more rapid recovery of longitudinal magnetization and, therefore, increased signal intensity on T1-weighted images. Consequently, better differentiation of brain tissue from veins is expected when the flip angle is increased, up to a point. This was observed in the images with 15–30° flip angles (Figs. 1 and 3). Increasing the flip angle to 60° decreased venous image quality, primarily owing to large saturation losses of the flowing spins. There were also larger signal contributions from other tissues, such as fat and contrast-enhancing structures (nasal mucous), obscuring the veins. A flip angle around 30° was found to be optimal for both the original and projection images.

The choice of TE was important since it indirectly affected the overall quality of the images. Changes in the TE did not

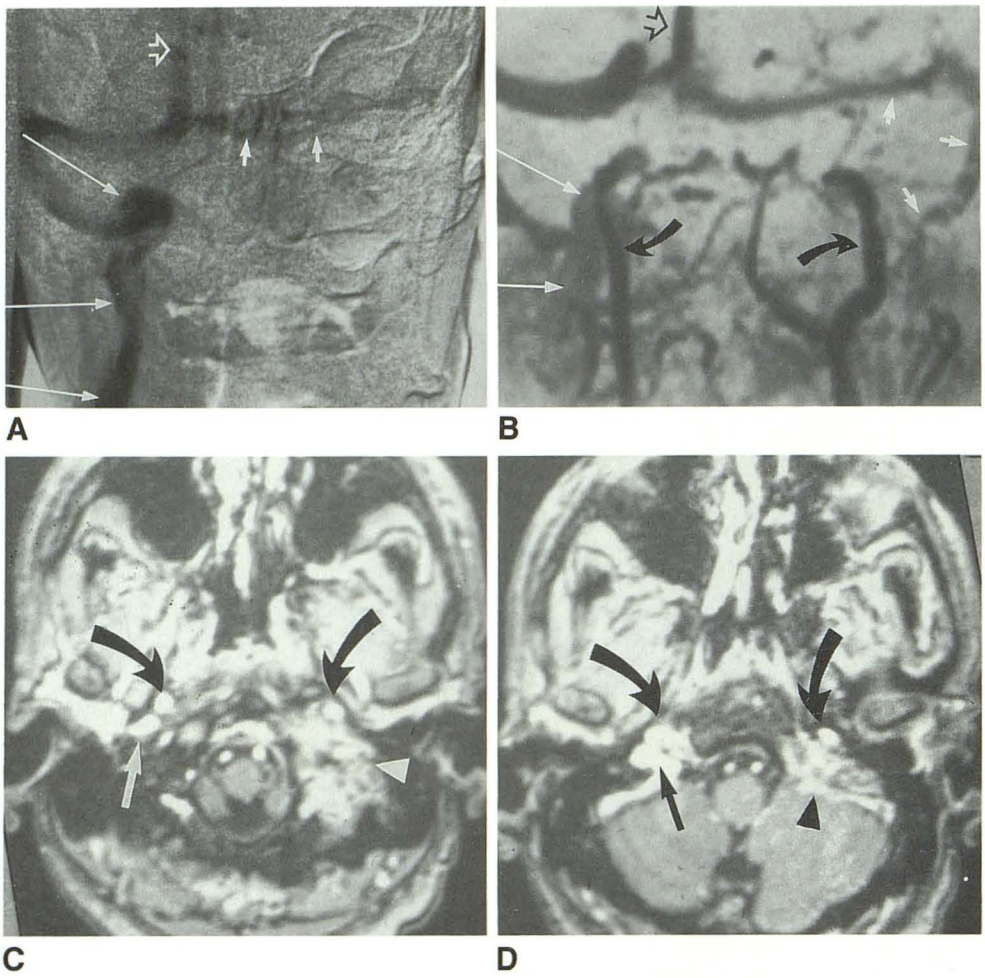

Fig. 11.—Comparison of standard and MR angiography of jugular occlusion in elderly man with a history of multiple left lower cranial nerve palsies, suggesting a jugular fossa lesion. Biopsy showed metastatic small cell carcinoma.

***A*, Anteroposterior digital subtraction angiogram from late venous phase of aortic arch injection shows complete occlusion of left jugular fossa and vein (*short white arrows*). *Open arrow* = superior sagittal sinus.**

***B*, Anteroposterior ray-tracing image from 3-D MR angiogram, contrast-enhanced axially acquired series, displays patent right jugular bulb and vein (*long white arrows*) and normal carotid arteries (*curved arrows*) with complete occlusion of left jugular vein (*shorter white arrows*). *Open arrow* = superior sagittal sinus.**

***C* and *D*, Axial slices from same series show tumor invading left jugular fossa (*arrowheads*) without involvement of adjacent brain or carotid arteries (*curved arrows*). *Straight arrows* = jugular veins.**

directly change the visualization of the venous structures, but rather they affected the regions containing fat and water (Fig. 7) [17]. TEs of 7 or 11 msec helped to suppress the fat signal, which can be a serious problem, particularly on ray-tracing images of the vertex of the skull. A TE of 7 or 11 msec corresponds with the antiparallel alignment of the fat and water magnetic vectors. For further image improvement it might be necessary to implement fat suppression in the image sequence.

The TE also may affect image contrast by dephasing effects, with potential loss of signal with longer TEs. Since image contrast is dominated in part by T1 effects, and since the venous flow is slow, signal loss due to dephasing for larger voxel sizes or longer TEs did not pose a significant problem, in contrast to arterial blood flow. For fast flow, larger voxel sizes yield lower signal, owing to the fact that the velocity distribution within the voxel causes spin dephasing. For more T1-based images and slow flow, however, larger voxels may yield improved signal to noise, and thus contrast to noise. Because the velocities of venous flow are slower than those of arterial flow, less higher-order motion is expected. Because of this, very short TEs are not as critical as they are with fast arterial flow to prevent spin dephasing [1]. On the other hand, the use of gadopentetate dimeglumine decreases not only T1 but also T2 relaxation, necessitating an appropriately short TE to prevent potential signal loss from the vascular structures.

The physiologic excretion and redistribution of the gadopentetate dimeglumine contrast material did have a profound effect on image quality. The 3-D MR angiographic contrast-enhanced study must be completed rapidly after injection, since a high concentration in the blood pool is crucial to ensure a good study (Fig. 4). The quality of the venous anatomy is maintained for a relatively long interval after injection (approximately 30 min). Repeat injections of contrast material may also be used to ensure adequate contrast enhancement, as long as the total dose does not exceed recommendations.

Physiologic time-of-flight effects of both the venous and arterial vessels are very important. Even with contrast enhancement, influx of unsaturated spins is a component of the signal characteristic. Choice of the overall imaging volume in relation to normal venous flow is crucial because of saturation effects. There was gradual loss of signal from the sagittal, transverse, and sigmoid sinuses and jugular bulbs on the more inferior sections of axially acquired images (Figs. 3, 9, and 11), secondary to progressive saturation of venous spins flowing into the inferior parts of the image volume, since the spins remain in the excitation volume for an extended time. Another example of this saturation phenomenon is the fact

that the jugular fossae were better seen on sagittally than on axially acquired images because of inflow of spins from the transverse sinuses (which are outside the sagittal excitation region) (Fig. 5). The same phenomenon may account for better visualization of the deep veins on axially acquired rather than sagittally acquired images, in which case the superior portion of the brain is not included in the imaging volume, and thus allows for inflow of unsaturated spins (Figs. 5, 8, and 9). We found that a total combination of the imaging volume, direction, and velocity of venous flow has significant effects on visualization of the small and large veins.

Review of the originally acquired and postprocessed images is also essential, since nonvisualization of veins on the projection images may be artifactual and technique dependent rather than a true finding of occlusion or other disease (Fig. 6) [14]. Because the stationary background tissue has relatively high signal, a vein may well be visible on the original image but not evident on the ray-tracing projection (Fig. 6).

The correlation between the cut-film angiograms and the MR angiograms is quite compelling. For example, the major dural sinuses are well seen on MR angiography without the problem of partial venous filling seen on the selective angiograms (Figs. 8–11). An aortic arch injection or a direct venous catheterization is frequently needed for more complete venous angiographic filling (Fig. 11). The deep venous system is also well seen on MR angiography, which has lower resolution than standard angiography, but the 3-D display and the ability to select the processed volume proved to be a major advantage. For example, if the dural sinuses obscure a small vessel on the standard angiogram, it may not be resolved (Fig. 8). On MR angiography, a rotated or regional volume view may accurately display the small vessel.

Limitations inherent to the maximum-intensity ray-tracing technique accounted for nonvisualization of small vessels (such as the septal veins), which were seen on the original images but not on the angiographic projections of large volumes (Fig. 6). The smaller the ray-tracing volume, the more detailed the depiction of the enhancing structures. Trimming the volume down could exclude regions that were not of interest or that were troublesome, such as the enhancing mucosa of the sinuses.

The quality of the original brain images alone is very good, so this MR angiographic technique could substitute for other T1-weighted spin-echo images, saving time (Fig. 8) [17]. The contrast is similar to that of T1-weighted spin-echo images. There is some loss of signal from magnetic susceptibility differences seen at bone, air, and brain interfaces, but the changes were not severe since the TEs were relatively short. Clear definition of contrast-enhancing disease was possible (Figs. 7, 10, and 11).

This MR angiographic technique has several major limitations. The 3-D technique is not ideal for visualization of the complete cerebral venous system. The present imaging volume is inadequate to include the complete head, and saturation is a major problem (Figs. 2 and 5). With this technique it would be necessary to acquire at least two different imaging volumes in which the venous territory is not completely encompassed to allow inflow of unsaturated spins. This is not as serious a limitation with 2-D time-of-flight techniques, since the imaging slice is small and there is little saturation effect. Also, saturation is not as serious a problem with phase-contrast imaging, where the complete head can be studied in one series.

Confusion of high-signal regions due to enhancement, other high-signal structures, and blood flow is a potentially serious problem (Figs. 3, 7, and 8) [18]. For example, an enhancing tumor may obscure a vascular stenosis, since the lesion may envelop the narrowed vessel, as when a superior sagittal sinus thrombosis is obscured by an enhancing falx meningioma. Confusion can also be caused by enhancement of normal tissues, including the dural structures, choroid plexus, nasal mucosa (Fig. 4), and other vascular structures without blood barriers (such as the pituitary stalk). Other high-signal tissues unaffected by contrast enhancement (such as scalp fat or subacute hemorrhage) also may be a problem [18]. An enhancing tumor in the location of normal venous channels could produce potentially confusing findings. Review of spin-echo or other images usually resolves the potential misinterpretation. Characterization of flow properties such as direction, quantitative velocity, and higher-order motion contributions is not obtainable with this technique. This is a disadvantage if physiologic information is desired.

Possible indications for venous MR angiography include dural sinus thrombosis, venous angioma, varix, unexplained cerebral hemorrhage, arteriovenous malformation, venous anomaly, jugular paraganglioma, giant jugular bulb, contraindication to routine angiography, and demonstration of the normal venous anatomy for surgical planning. Complete assessment of both the venous and the arterial anatomy is important. If MR angiography is to be used for more than just a rough screening examination, extensive and consistent visualization of the entire cerebral vascular system is necessary.

In summary, unenhanced single-excitation 3-D MR angiography is quite insensitive in the evaluation of cerebral venous structures. Contrast enhancement allows for rapid scanning times and excellent visualization of most of the important venous anatomy. We documented good correlation of cut-film angiograms and MR angiograms. This technique could be used as a venous screening examination and could also substitute for a T1-weighted enhanced study so that the total examination time would not be seriously lengthened. We found the best image quality was obtained with a 50/7/30° sequence.

REFERENCES

1. Nishimura DG, Macovski A, Pauly JM. Considerations of MRA by selective inversion recovery. *Magn Reson Med* **1988**;7:472–484
2. Dumoulin CL, Cline HE, Souza SP, Wagle WA, Walker MF. 3-D time of flight MRA using spin saturation. *Magn Reson Med* **1989**;11:35–46
3. Laub GA, Kaiser WA. MR angiography with gradient motion refocusing. *J Comput Assist Tomogr* **1988**;122:377–382
4. Dumoulin CL, Hart HR. Magnetic resonance angiography. *Radiology* **1986**;161:717–720
5. Dumoulin CL, Souza SP, Walker MF, Wagle W. Three-dimensional phase contrast angiography. *Magn Reson Med* **1989**;9:139–149
6. Ruggieri PM, Laub GA, Masaryk TJ, Modic MT. Intracranial circulation: pulse sequence considerations in three-dimensional (volume) MR angiography. *Radiology* **1989**;171:785–791
7. Masaryk TJ, Modic MT, Ross JS, et al. Intracranial circulation: preliminary

clinical results with 3-D (volume) MRA. *Radiology* **1989**;171: 793–799
8. Gullberg GT, Wehrli FW, Shimakawa A, Simons MA. MR vascular imaging with a fast gradient refocusing pulse sequence and reformatted images from transaxial sections. *Radiology* **1987**;165:241–246
9. Keller PJ, Drayer BP, Fram EK, Williams KD, Dumoulin DL, Souza SP. MR angiography via 2-D acquisition and three-dimensional display. Work in progress. *Radiology* **1989**;173:527–532
10. Hale JD, Valk PE, Watts JC, et al. MR imaging of blood vessels using three-dimensional reconstruction: methodology. *Radiology* **1985**;157: 727–733
11. Wedeen VJ, Mueli RA, Edelman RR, Frank LR, Brady TJ, Rosen BR. Projective imaging of pulsatile flow with magnetic resonance. *Science* **1985**;230:946–948
12. Masaryk TJ, Ross JS, Modic MT, Lenz GW, Haacke EM. Carotid bifurcation: MR imaging. *Radiology* **1988**;166:461–466
13. Tsuruda J, Halbach VV, Higashida RT, Mark AS, Hieshima GB, Norman D. MR evaluation of large intracranial aneurysms using cine low flip angle gradient-refocused imaging. *AJNR* **1988**;9:415–424
14. Anderson CM, Saloner D, Tsuruda JS, Shapeero LG, Lee RE. Artifacts in maximum-intensity-projection display of MR angiograms. *AJR* **1990**; 154:623–629
15. Wehrli FA, Perkins DG, Shimakawa A, et al. Chemical shift induced amplitude modulations in images obtained with gradient refocusing. *Magn Reson Imaging* **1987**;5:157–158
16. Edelman RR, Mattle HP, Kleefield J, et al. Quantification of blood flow with dynamic MR imaging and presaturation bolus tracking. *Radiology* **1989**;171:551–556
17. Steinberg PM, Ross JS, Modic MT, Tkach J, Masaryk TJ, Haacke EM. The value of fast gradient-echo MR sequences in the evaluation of brain disease. *AJNR* **1990**;11:59–67
18. Yousem DM, Balakrishnan J, Debrun GM, Bryan RN. Hyperintense thrombus on GRASS MR images: potential pitfall in flow evaluation. *AJNR* **1990**;11:51–58